THE HELIUM ATOM MICROSCOPE - REPORT ; 3

(1/4/92 - 14/6/92)

J. Lower

Table of Contents

Abstract

Two and a half months after the completion of report number 2, the perspective has again dramatically changed in light of both new information and better understanding of the problems to be confronted. The design constraints appear now well established and in this essay I present, for the first time, a microscope design in detail, predict it's performance and assess it's prospects for future improvement. It must now be deceided, upon the information presented here, whether the design warrants proceeding to the construction stage.

In Chapter 1 I discuss the factors limiting the maximum atom current which can be focussed, through the agency of a Fresnel lens, down to a microscopic spot on the target surface. The deleterious effects of finite source size are explained in the context of a high pressure helium nozzle expansion. After calculating the focussed atom flux obtainable at a resolution of 0.4 μ for a low temperature helium beam, a comparison is made with the performance of a simple lensless microscope design.

From Chapter 1 it becomes clear that due to the expected low primary beam intensities, the feasibility of the microscope hangs upon the level of atom detection efficiency which can be reached. Chapter 2 therefore describes ways in which the performance of existing detectors can be improved for the specific application of use in an atom microscope. Also discussed are factors determining maximum scan rate for a particular microscope design and in context, the concept of an optimum detector stagnation pressure.

A short conclusion is presented in Chapter 3.

1. Optimization of Primary Beam

1.1 Experimental Setup

The proposed design for the generation of the focussed incident beam is shown in Figure 1.1 below.

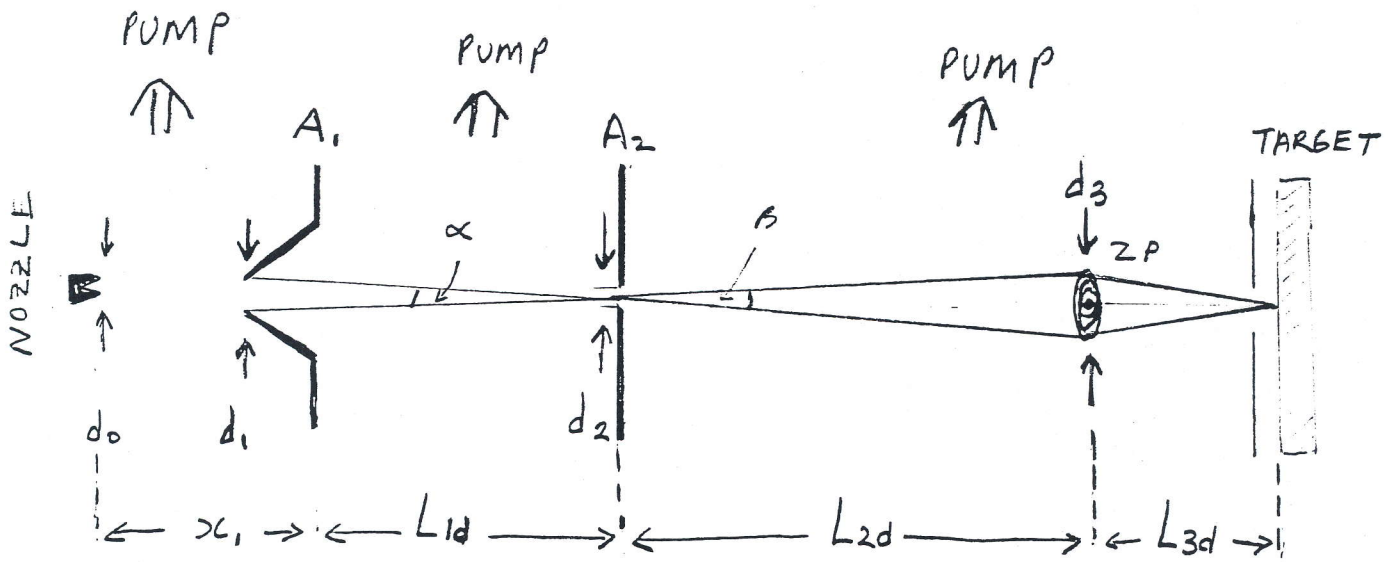

Figure 1.1

A high intensity, highly monochromatic helium beam is produced by the supersonic expansion of gas, at high pressure, through a small aperture of diameter d_0. A skimmer A_1 of diameter d_1 and at a distance x_1 downstream from the nozzle serves to select a narrow, forwardly directed atom beam. Furthermore, the skimmer restricts background pressure in the second chamber, thereby limiting collisions between beam and background atoms over the relatively large distance L_{1d} to the much smaller aperture A_2 downstream. The aperture A_2, diameter d_2 serves as a small atom source, a demagnified image of which is formed by the zone plate on the target surface. The ratio of skimmer diameter d_1 to the distance L_{1d} defines the angle α shown in the diagram. The zone plate ZP of diameter d_3 is located a distance L_{2d} downstream from aperture A_2. The distance L_{2d} is determined by the chosen microscope demagnification factor M and the intrinsic focal length of the

zone plate for a given source temperature T_0 (see report number 2). The angle β shown is determined by the ratio d_3/L_{2d}. The Microscope resolution will be determined by the intrinsic resolution of the zone plate, the aperture diameter d_2 and the demagnification factor M. It is the magnitude of the atom current $\dot{N}$ incident upon the zone plate surface which, in combination with the detector efficiency, will determine the ultimate microscope count rate.

I note that diffraction of the helium atoms, as they pass through the small aperture A_2, will result in not insignificant broadening of a cold atom beam relative to the dimensions of the zone plate itself. From Optics [1], the full width at half maximum of the intensity distribution of a plane wave truncated by an aperture of diameter d at a screen a distance L away is given by the expression:

$$\Delta = 1.22 \frac{L\,\lambda}{d} \quad metres \tag{1.1}$$

where λ is the atom wavelength. In the example to follow, Δ is 30 μ for $L_{2d} = 48$ cm (corresponding to a demagnification factor of five), a helium wavelength of $\lambda = 1\mathring{A}$ and aperture diameter $d_2 = 2\mu$.

1.2 Intensity Calculations

As an illustration of what could realistically be expected from such a configuration, in terms of the focussed beam intensity for a given resolution, I assume the following set of parameter values and make the following assumptions in the calculations to follow:

(a) Using a helium source pressure P_0 of 80 bar, a source temperature T_0 of 78 °K and a nozzle diameter d_0 of 10 μ Bruce Doak [2] obtained a measured velocity spread $\Delta v/v =$ .6 % i.e. a speed ratio of 275. I assume these parameter values in the present calculation as

they represent the best I have seen reported for a high intensity, high monochromaticity, low temperature helium beam for the present application. All on axis intensities are calculated using the formulae of Knuth [3].

In passing I note that the effective source size, intrinsic in the theory of Knuth [3], relies upon the assumption that

$$\Delta v_{\perp}/v_{\perp} = \Delta v_{\parallel}/v_{\parallel}. \tag{1.2}$$

at the sudden freeze surface (see Figure (1.2)). For the beam parameters above however, Bruce Doak measured a much larger value for the perpendicular as the parallel velocity spread. This measurement must cast some doubt on the theoretical predictions for intensity in the present case for the following reason. In normal atom diffraction experiments, where agreement between theoretical and experimental intensities has been well established, the perpendicular velocity distribution at the sudden freeze surface has no significant bearing upon the beam intensity at a distant observation point. It is only when one introduces extremely small apertures in the beam path that this factor plays a paromount role in determining on axis beam intensity. Therefore, agreement between predictions of theory and experiment under normal conditions for atom diffraction experiments does not necessarily imply agreement will exist in our particular geometry.

(b) A nozzle skimmer distance x_1 of 2 cm is assumed. The distance R_f to the sudden freeze surface for a nozzle diameter d_0 and a Mach number M_T is given by [2]:

$$R_f \simeq [\frac{M_T}{A}]^{\frac{1}{\gamma-1}} \quad metres \tag{1.3}$$

where γ is the ratio of specific heats (1.63 for Helium) and A is a constant (3.26 for He). For a nozzle diameter d_0 of 10 microns and a Mach number M_T of $\simeq$ 300 in Doak's

experiments, the calculated distance to the sudden freeze surface is then 8 mm. Therefore, it may be possible to position the skimmer closer to the nozzle than is presently assumed, thereby gaining an increase in intensity, the size of which is given by equation (1.6) (see pg. 9). However, the requirement of low background pressure around the nozzle to avoid degredation in beam flow characteristics may preclude reductions in the distance x_1 from the present assumed value.

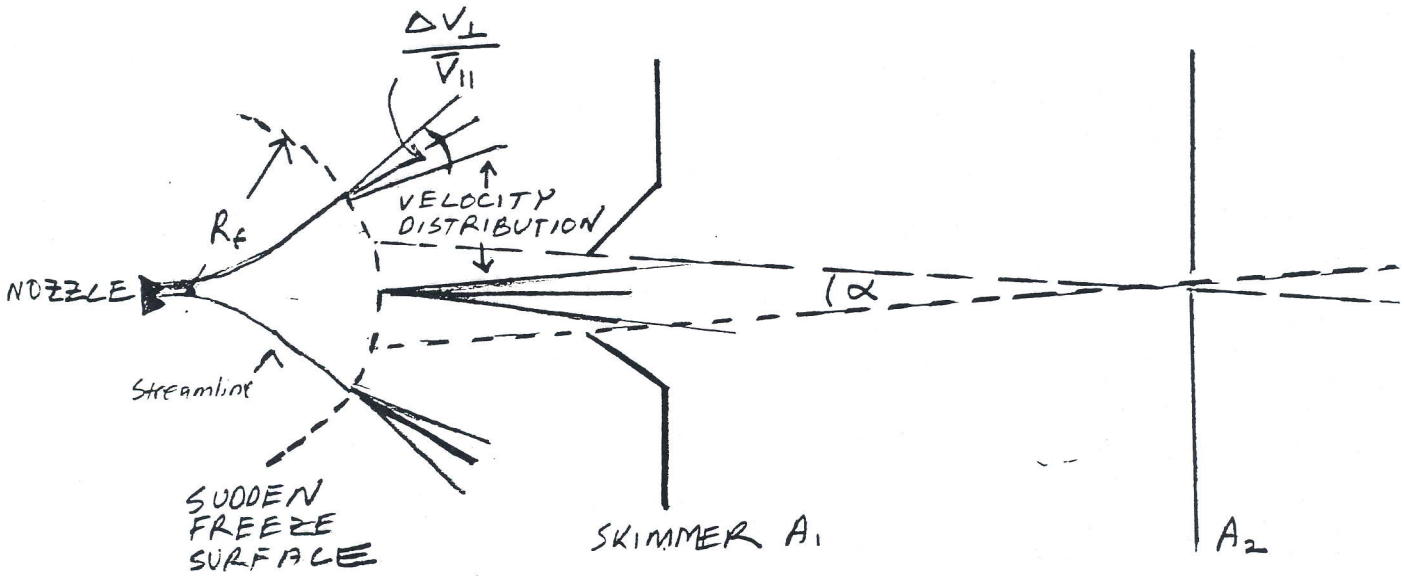

Figure 1.2

(c) I assume a zone plate diameter of 80 microns diameter with outer ring thickness of .1 micron, focal length of 8 cm at liquid nitrogen temperatures (i.e atom wavelength of 1.0 Angstroms) and an intrinsic resolution of .14 micron. These parameters correspond to the best free standing zone plate the X-ray Physics Group, Gottingen, predict they could make.

(d) A diameter of 2 microns for aperture A_2 in conjunction with a demagnification of a factor 5 to give a total microscope resolution of $\simeq$ .42 microns. Distance L_{2d} is then fixed at 48 cm. Furthermore, I assume a skimmer diameter of D_1 of 100 microns and assume that the angles α and β in figure 1 are related by the relation $\alpha = 2\beta$ (Justification given in Appendix 1). L_{1d} is then fixed at 32 cm.

With these assumptions, I calculate intensity with the following formulae [3]:

(1) The ideal gas law to calculate the density n_0 in the source at temperature T_0 and pressure P_0 i.e.

$$\begin{aligned} n_0 &= \frac{P_0}{kT_0} \\ &= \frac{85 \times 1.05 \times 10^5}{1.38 \times 10^{-23}} \\ &= 7.32 \times 10^{27} \quad m^{-3} \end{aligned} \tag{1.4}$$

(2) The atom density n_1 at the skimmer entrance, a distance x_1 away from the nozzle, is related to the atom density n_0 in the source by the expression:

$$\begin{aligned} n_1 &= 0.156\,(\frac{x_1}{d_0})^{-2} n_0 \\ &= 0.156 \left(\frac{2 \times 10^{-2}}{10 \times 10^{-6}}\right)^{-2} \times 7.32 \times 10^{27} \\ &= 2.85 \times 10^{20} \quad m^{-3} \end{aligned} \tag{1.5}$$

where d_0 is the nozzle dimension.

(3) The atom density n_d at aperture A_2 is related to the density n_1 at the skimmer entrance by the expression:

$$\begin{aligned} n_d &= n_1(\frac{x_1}{L_{1d}}^2)\left[1 - e^{-S_1{}^2 sin^2 \xi_{max} cos^2 \xi_{max}}\right] \\ &= 2.85 \times 10^{20} \left(\frac{2 \times 10^{-2}}{62.5 \times 10^{-2}}\right)^2 \times 0.38 \\ &= 1.10 \times 10^{17} \quad m^{-3} \end{aligned} \tag{1.6}$$

where S_1 is the beam speed ratio and ξ_{max} is the angle from nozzle to skimmer lip.

Choosing $\alpha = \beta$ ($\xi_{max} = 2.5 \times 10^{-3}$ *radians*) and for a speed ratio $S = 275$ as reported by Doak [2], the factor $[1 - e^{-S_1{}^2 sin^2 \xi_{max}} cos^2 \xi_{max}] = 0.38$. This factor accounts for the reduction in intensity at A_2 due to the presence of the skimmer and would indeed be 1.0 if no skimmer were present. Therefore in the present example, the emitting surface seen at A_2 would be more than 100 μ in the abscence of the skimmer. In other words, the effective source size is much larger than the nozzle dimension in the case of a high pressure gas expansion through a small nozzle. That the effective source size is much larger than the nozzle aperture greatly limits the amount of atom current which, for a given resolution, can be focussed onto the target surface. However, under the assumed beam parameters Doak [2] measured the effective souce size to be 500 μ. If he is right, then the calculated intensities to follow will be a factor $\simeq 5$ or more too high ! Note that the effect of reducing x_1 from 20 to 10 mm, proposed earlier as a possible improvement, would only increase n_d by a factor of 2.2 from the above equation for the present parameter values.

For the proposed design, the angle α is chosen to be 2 times larger than β, not $\alpha = \beta$ as assumed above. This choice results in a slightly improved value of atom number density at the zone plate. Indeed, the component of the atom number density $n_d{}^*$ at aperture A_2 which contributes to intensity at the zone plate is calculated as:

$$n_d{}^* = 1.3 \times 10^{17}\ m^{-3} \tag{1.7}$$

The method by which this number was determined is described in Appendix 1. To obtain the number of atoms per second N focussed onto the target surface, $n_d{}^*$ must be multiplied by the beam velocity $v_{\|}$, the area $\frac{\pi}{4} d_2{}^2$ of the aperture A_2 and divided by a factor 20 to account for the fact that only 5 % of atoms incident upon the apodised zone plate are focussed into the first order diffraction peak. The beam velocity $v_{\|}$ is related to the source temperature through the expression:

$$
\begin{aligned}
v_{\parallel} &= \left[\frac{5\ k\ T_0}{m}\right]^{\frac{1}{2}} \\
&= \left[\frac{5 \times 1.38 \times 10^{23} \times 78}{4 \times 1.67 \times 10^{-27}}\right] \\
&= 922\ \ m\ s^{-1}
\end{aligned}
\tag{1.8}
$$

Thus:

$$
\begin{aligned}
\dot{N} &= \frac{\pi}{80} v_{\parallel} {d_2}^2 {n_d}^* \\
&= \frac{\pi}{80} \times 922 \times {d_2}^2 \times 1.3 \times 10^{17} \\
&= 1.9 \times 10^7\ \ sec^{-1} \qquad (at\ .4\ \mu\ resolution)
\end{aligned}
\tag{1.9}
$$

I note that by reducing the diameter of aperture A_2 to 1 μ, for the same demagnification, a resolution of .23 μ would be achieved with a concomitant factor 4 reduction in beam intensity. Reducing the aperture diameter to .5 μ, a resolution of .16 μ would be achieved with a factor 16 reduction in intensity. Here I have used the intrinsic zone plate resolution of .122 μ in quadrature with the demagnified aperture size A_2/M to calculate the total resolution.

Finally, the microscope resolution depends not only upon the diffraction limited resolution of the zone plate, the size of the source aperture A_2 and the chosen demagnification factor M but also upon the angle at which the beam impinges upon the target surface, as the calculated spot size is a measure of the microscope resolution only in the case of normal incidence. By projecting the spot onto a surface whose normal is at an angle η to the beam direction, the spot lengthens by a factor $\frac{1}{cos(\eta)}$ and the resolution degrades by a corresponding factor.

1.3 Pinhole Microscope

At this point it is interesting to compare the amount of flux delivered onto the target surface, for a given resolution, by the Fresnel lens microscope described above and one consisting simply of an illuminated pinhole positioned close above the target surface. This lensless microscope is shown schematically in Figure 1.3.

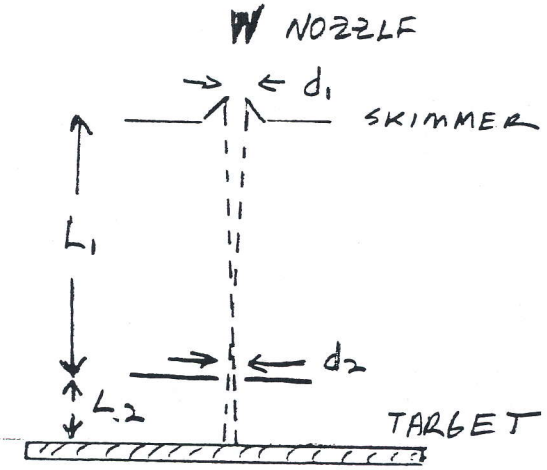

Figure 1.3

I assume here, for the sake of comparison, the same atom source employed in the preceeding calculations. i.e. a 10 μ diameter nozzle through which helium at 80 bar pressure and at a temperature of 78 ° K expands, positioned 20 mm behind a 100 μ skimmer. The size of the illuminated target area depends upon five factors, namely the skimmer diameter d_1 and it's distance L_1 from the pinhole P, the pinhole diameter d_2 and the distance L_2 from pinhole to target surface and the wavelength λ of the illuminating atom beam. The total microscope resolution δ_{tot} is given approximately by the expression:

$$\delta_{tot} = \left[\left(d_1 \cdot \frac{L_2}{L_1}\right)^2 + (d_2)^2 + \left(1.22\,\frac{L_2\,\lambda}{d_2}\right)^2 \right]^{\frac{1}{2}} \quad metres \tag{1.10}$$

The first term in the main brackets accounts for demagnification of the source due to the differences in distances L_1 and L_2 (see dashed lines in figure), the second term accounts for

the finite size d_2 of the pinhole itself and the third term accounts for resolution broadening due to diffraction of atoms through the pinhole (see equation (1.1)). Taking as an example, a pinhole size d_2 of .5 μ (the smallest commercially available aperture of which I am aware), a distance L_1 from skimmer to pinhole of 20 cm and a distance L_2 from pinhole to target surface of 1 mm, equation (1.10) yields:

$$\begin{aligned} \delta_{tot} &= \sqrt{0.5\ \mu^2 + 0.5\ \mu^2 + 0.25\ \mu^2} \\ &= 0.78\ \mu \end{aligned} \tag{1.11}$$

From equations (1.6) and (1.9), the number of atoms per second $\dot{N}$ passing through aperture P onto the target surface is 2.4×10^8 atoms/second. This corresponds to an improvement in atom flux of a factor of $\simeq$ 3.5 when compared to that which would be achieved with a zone plate for the same resolution i.e. by choosing the aperture diameter A_2 as 4 rather than 2 μ (see figure 1.1). Inspection of equation (1.10) shows that to obtain a factor 2 improvement in resolution one could halve the pinhole diameter d_2 and either halve the distance L_2 of the pinhole to the surface or double the skimmer to pinhole distance L_1 and use a beam of twice the temperature to reduce the size of the diffraction term $(1.22\ \frac{L_2\ \lambda}{d_2})^2$ in equation (1.10). If the alternative of moving the source back and choosing a smaller aperture and higher source temperature is chosen, then a factor of 16 reduction in intensity follows for every factor 2 improvement in resolution ! In contrast, the alternative of halving the distance L_2 in combination with a smaller aperture size A_2 results in only a factor 4 reduction in intensity. However, to bring the pinhole P extremely close to the target surface introduces severe practical difficulties in terms of interference of the pinhole mount with the scattered signal.

2. Optimization of Atom Detector

2.1 Fundamentals

The final microscope count rate $\dot{q}$ will depend upon the detector performance as well as the characteristics of the incident beam. It's value is given by the product of the detector ionization efficiency $\zeta(x,y,z,T)$ (ions/torr/m^{-3}/sec) and the helium pressure $P(x,y,z,\frac{d\sigma(\theta,\phi)}{d\Omega},\dot{N},T)$ integrated over the ionization volume, where T is the temperature of the gas in the ionization region. Here $\frac{d\sigma(\theta,\phi)}{d\Omega}$ is the differential scattering cross section for scattering from the point under observation on the target surface. It is the point to point variations in this quantity which gives rise to image contrast. $\dot{N}$, as before, is the number of helium atoms per second incident upon and reflected from the target surface. Thus

$$\dot{q} = \int_{Detector} \zeta(x,y,z,T)\ P(x,y,z,\frac{d\sigma(\theta,\phi)}{d\Omega},T,\dot{N})\ dx\,dy\,dz \tag{2.1}$$

In the case where molecular flow conditions prevail in the detector we can write

$$P(x,y,z,\frac{d\sigma(\theta,\phi)}{d\Omega},T,\dot{N}) = \chi(x,y,z,T,\frac{d\sigma(\theta,\phi)}{d\Omega})\cdot\dot{N} \tag{2.2}$$

where χ is the pressure distribution in the detector normalized for an atom throughput of one atom per second i.e.

$$\dot{q} = \dot{N}\cdot\int_{Detector} \zeta(x,y,z,T)\ \chi(x,y,z,T,\frac{d\sigma(\theta,\phi)}{d\Omega})\ dx\,dy\,dz \tag{2.3}$$

With an unmodified detector of the type generally used for surface diffraction studies, the coefficient relating $\dot{q}$ and $\dot{N}$, given by the integral, would be less than 10^{-7}. Thus for a value $\dot{N} = 1.9 \times 10^6$ atoms/sec (equation (1.9)) a count rate of only $\simeq 0.1$ Hz would be expected !! The reasons for this poor result are three fold:

(a) For atoms passing through the ionization region, the ionization efficiency of these detectors is very small ($\simeq 10^{-5}$).

(b) Only atoms leaving the surface through a very small solid angle will pass through the ionization region due to it's particular geometry (developed for detection of narrow parallel beams of atoms) and the fact that the physical size of the detector limits how close the ionization region can be brought to the the target. For a helium atom microscope, detection of scattered atoms over a large solid angle will be required to achieve acceptable levels of count rate.

(c) Atom detectors used in surface diffraction studies are usually "flow through" type detectors, meaning that atoms pass through the ionization region only once before leaving through the exit aperture.

Although these points together paint a bleak picture, the requirements for a microscope detector are sufficiently different from those for a detector used for time resolved surface studies to allow substantial improvement in ionization efficiency to be wrought. The use of a "magnetic bottle" type of detector, of the type tested by von Issendorff [4], is one way to gain improved sensitivity. In this type of detector, electrons are confined to the ionization region by a magnetic field, the electron density in this region and hence the ionization efficiency being thereby substantially increased. Such a detector is not applicable to high resolution time resolved measurements due to it's intrinsically long ($\tau \simeq 10\ \mu$) time constant. For microscope applications, however, this response time could indeed be fast enough and the reported factor of 20 in ionization efficiency over conventional ionization detectors utilized [4].

Another means to obtain improved ionization efficiency is to "stagnate" the ionization detector. In this mode the detector is completely enclosed, except for an entrance aperture to accept incoming neutral atoms and an exit aperture for the extraction of helium ions. Atoms enter the detector, undergo many collisions with the detector walls and traverse the ionization volume many times before finally leaving, the extent of pressure build up in the detector being determined by the size of the apertures [Appendix 2]. The increase in sensitivity is again achieved at the expense of detector speed, however by making the detector volume sufficiently small, acceptably fast response times can be achieved for microscopy applications.

The resultant pressure build up P_∞ in the detector itself will depend upon the temperature T_0 and throughput $Q(T_0)$ of gas entering the detector, the temperature T of the detector and the total conductance $C(T)$ of the detector apertures. These quantities are related through the expression:

$$P_\infty = \frac{Q(T_0)}{C(T)} \cdot \frac{T}{T_0} \quad torr \tag{2.4}$$

The response time τ of the detector depends upon it's volume V and the conductance $C(T)$ of the apertures for a particular detector temperature T [Appendix 2]:

$$\tau = \frac{V}{C(T)} \quad seconds \tag{2.5}$$

Here I have neglected the intrinsic time delay between the ionization of atoms and their removal from the detector volume, a quantity which will vary from detector to detector.

For the present application, the conductance C of the detector will be dominated by the diameter d of the ion exit aperture as the entrance aperture, if positioned close to the

target surface, can be made extremely small whilst still enabling collection of atoms over a large solid angle as all scattered atoms emerge from a microscopic point upon the surface. The conductance of a circular aperture of diameter d (measured in metres) for a gas of temperature T and molecular weight M is given by the expression [5]:

$$C = 2.91 \times 10^4 \left(\frac{T}{M}\right)^{\frac{1}{2}} \cdot d^2 \ \ litres/sec. \tag{2.6}$$

To illustrate the level of count rate attainable with existing technology, I take as an example the magnetic detector of von Issendorff operated in stagnation mode. For this detector, the exit ion aperture diameter is 5 mm diameter, the detector volume 25 cm^3 and the operation temperature 300 $^\circ K$. I assume that the detector is encapsulated, except for the presence of entrance and exit apertures and 10 % of flux scattered from the surface is collected through the agency of an entrance cone. This corresponds to a collection angle α of 46 % if isotropic scattering is assumed. In the case of a stagnation detector, the pressure will be essentially constant throughout the ionization volume and hence equation (2.1) simplifies to:

$$\dot{q} = P\ (\frac{d\sigma(\theta,\phi)}{d\Omega}, T, \dot{N}) \cdot \int_{Detector} \zeta(x,y,z,T)\ \ dx\, dy\, dz \tag{2.7}$$

Here I have assumed that the degree of stagnation is relatively high and no "tricks" in design have been employed to introduce pressure gradients to improve count rate [Appendix 3]. By introducing Helium into the experimental chamber of a specific pressure $P(\frac{d\sigma(\theta,\phi)}{d\Omega}, T, \dot{N})$, the factor

$$\zeta_{int}(T) \ = \int_{Detector} \zeta(x,y,z,T)\ \ dx\, dy\, dz \ \ \ torr^{-1}\ second^{-1} \tag{2.8}$$

can be determined by measuring the total ion current $\dot{q}$. In this way, von Issendorff [4] measured $\zeta_{int}(T)$ to be 7.5×10^{15} $ions/torr/sec$ at room temperature. Note that because the ionization rate scales in proportion to atom number density in the ionization volume, which in turn scales with the gas temperature for a given volume, we can deduce $\zeta_{int}(T)$ for all temperatues from the room temperature measurement by the relation:

$$\begin{aligned} \zeta_{int}(T) &= \zeta_{int}(300^{\circ}K) \cdot \frac{300\ ^{\circ}K}{T\ ^{\circ}K} \\ &= \frac{(2.25 \times 10^{18})}{T} \quad ions/torr/second \end{aligned} \tag{2.9}$$

The final quantity to calculate, before the count rate can be derived from equation (2.7), is the atom throughput in $torr - litres/sec$ entering the detector. Using equation (1.4), the number of atoms N_{t-l} in a torr-litre at temperature T_0 is given by:

$$\begin{aligned} N_{t-l} &= \frac{[(1.01 \times 10^5 \times \frac{1}{760}] \times 10^{-3}}{1.38 \times 10^{-23}} \cdot \frac{1}{T_0} \\ &= \frac{9.63 \times 10^{21}}{T_0} \quad atoms \end{aligned} \tag{2.10}$$

Thus

$$\dot{N} \quad atoms/second \ = \ 1.04 \times 10^{-22} \cdot T_0 \cdot \dot{N} \quad Torr - litres/second$$

So, using (2.4), (2.6) and (2.7),

$$\dot{q} \ = \ \frac{Q(T_0)}{C(T)} \cdot \frac{T}{T_0} \left(\frac{2.25 \times 10^{18}}{T}\right) \tag{2.11}$$

$$= \left[\frac{1.04 \times 10^{-22} \cdot T_0 \cdot \sqrt{M}}{2.91 \times 10^4 \sqrt{T} \cdot d^2 \cdot T_0}\right] \cdot (2.25 \times 10^{18}) \cdot \dot{N}$$

$$= (1.61 \times 10^{-8}) \cdot \left[T^{-\frac{1}{2}}\ d^{-2}\ \dot{N}\right] \tag{2.12}$$

$$= (3.7 \times 10^{-5}) \cdot \dot{N}$$

$$= 70 \quad ions/second$$

Due to the presence of an array of field correcting apertures within the detector, the actual conductance of the volume is likely to be $\simeq 2$ times lower than the value calculated solely on the basis of the circular exit aperture (equation (2.6)). Hence the stagnation pressure and ion count rate would also then be 2 times higher i.e. The expected count rate is thus more likely:

$$\dot{q} \simeq 140 \quad c/s \qquad (\text{at } .42\ \mu) \tag{2.13}$$

The time constant τ, for a detector volume V of 25 cm^3 and an exit aperture of 5 mm diameter (factor 2 correction for internal field correcting apertures again assumed) is, from equations (2.5), (2.6):

$$\tau = 7.9\ milliseconds \tag{2.14}$$

However, I note that it should be possible to considerably reduce the diameter of the field correcting apertures for this detector, bringing the detector volume down to approximately 10 cm^3 with a consequent improvement in time constant by a factor $\simeq 2.5$.

2.2 Scan Rate Considerations

In this section I address the question of what constitutes an optimum scan rate for a given microscope design and describe the factors limiting the maximum scan rate permissible.

Suppose that the intensity and minimum spot size for the incident beam are determined, as is the acceptance solid angle of the detector and the choice of target. In such a case, the image contrast and resolution of the microscope are determined in the limit that the dwell time T at each point is much larger than the response time τ of the detector (The scan speed υ (points/sec) then being simply T^{-1}). As T is reduced towards a value close to τ the image contrast and resolution both begin to degrade. The reason is that a certain fraction φ of signal derived from each scan point corresponds to the ionization of atoms which entered the detector at previous scan points but which have not yet left the detector. The maximum scan speed υ_{max} is therefore determined by the relation:

$$\upsilon_{max} = \frac{1}{T_{min}} = \frac{1}{K(\varphi) \cdot \tau} \tag{2.15}$$

where $K(\varphi)$ is a parameter determined by the largest value for φ acceptable. Thus

$$T > T_{min} = K(\varphi) \cdot \tau \tag{2.16}$$

For example, it can be shown [Appendix 4] that at any scan point, the signal contribution from previous points is less than 10 % ($\varphi = .1$) when the coefficient $K(\varphi)$ in equation (2.15) is greater than 5.0. Thus for a detector time constant τ of 20 milliseconds, for example, this condition would correspond to a maximum of 10 scans points per second.

From an entirely different perspective, to obtain an image of sufficient statistical quality δ for a given image contrast, the total dwell time T at each point must to be long enough to collect the N counts necessary where N, δ and T are related through the relation:

$$\begin{aligned} \delta &= \frac{\sqrt{N}}{N} \\ &= \frac{1}{\sqrt{N}} \\ &= (\dot{N} \cdot T)^{-\frac{1}{2}} \end{aligned} \tag{2.17}$$

i.e. We require

$$T > \frac{1}{\dot{N} \cdot \delta^2} \tag{2.18}$$

Whether this time interval is built up from many small time segments by scanning over the same target region many times or whether each point is scanned over only once has no bearing upon the time required to build up the image to the required accuracy. Thus, if it turns out that the minimum value for T calculated from equation (2.18) is greater than T_{min} from (2.16), then it makes sense to stagnate the detector further, thereby increasing the microscope count rate, to a stage where the value of T given by both equations is equal i.e. It is best to build up the image by scanning over each point only once, rather than many times, for a given total image accumulation time, thereby allowing the detector to be operated with the highest stagnation pressure possible and consequently the highest detection efficiency. In this way a spectrum satisfying the two requirements of a specified statistical accuracy δ and a specified maximum degredation to resolution and contrast from the finite time response of the detector, is formed in the minimum time. Of course, to scan only once over each point is only sensible if the experimental conditions remain extremely

stable over the duration of the experiment, as multiple scanning will always produces the favourable result of averaging over the effects instrumental drifts.

2.3 Further Scope for Improved Performance

The best way to improve the microscope count rate would be to produce a more intensive focussed incident beam. The reasons are twofold. Firstly, although much room exists for the improvement in detector ionization efficiency, increasing the sensitivity to helium necessarily increases the sensitivity to background gases which, depending upon the finite mass resolution of the mass spectrometer employed, may contribute to significant background levels in the measured spectra. Secondly, improving detector ionization efficiency, as demonstrated, may well be at the expense of detector response time, any increase in which reduces the maximum scanning speed possible. Unfortunately, for high pressure gas expansion through a nozzle, the finite velocity spread of beam atoms perpendicular to the flow direction, the onset of cluster formation at higher source pressures and limitations of pumping speed suggest the development of an improved zone plate as the only practical means to obtain higher incident beam intensities. The possibility of producing a large area reflecting zone plate to obtain higher intensities is discussed at a later point [Appendix 5]. I note however that by processing derived signal in software, a good scanning speed in spite of a long detector time constant may still be possible [Appendix 6]. Also presented in this Appendix are some ideas for a novel detector design.

Equation (2.12) shows two further ways to achieve achieve improved ionization efficiency. The simplest is to cool the detector, the stagnation pressure and hence the count rate improving as $\frac{1}{\sqrt{T}}$. Thus cooling to liquid nitrogen temperature (assuming the enclosed helium gas equilibrates to the detector wall temperature) would produce a factor 2 increase and cooling to close to liquid helium temperature a factor 8 improvement in count rate for the present case. Cooling the detector walls has the added advantage of condensing

out background gas from the detector volume producing considerable reductions in background signal, an effect which could be of crucial importance given the low helium partial pressures present. The second possibility is to reduce the exit aperture d used to extract ions from the detector and thereby increase the stagnation pressure. Considerable gains can in theory be made as the stagnation pressure improves as $\frac{1}{d^2}$, however any restriction of this aperture is likely to obstruct the ion current from leaving the detector. In principle however, I see no reason why an accelerating lens cannot be designed to defocus the ions from the exit aperture through a much smaller ($1 \rightarrow 2\ mm$) aperture, this second aperture now determining the stagnation pressure. Of course, the volume between the two aperture will increase the total detector volume and hence would have to be kept as small as possible to avoid significant increases in detector response time τ. Nevertheless, a decrease in aperture size from 5 mm to 2 mm would produce a factor 6.3 in stagnation pressure and hence count rate. Computer simulations need to be performed to determine the feasibility of this approach.

3. Conclusion

Due to the dynamics of high pressure helium expansion through a nozzle, our requirement for a cold, highly monochromatic helium beam, the constraints of finite pumping speed and the onset of cluster formation at higher source pressures and lower source temperatures, it appears that the best chance of improving the microscope focussed incident beam intensity is the development of an improved zone plate. However, the increasing difficulty of producing such lenses with ever finer structure suggests the development of a helium atom detector, of ionization efficiency much higher than is presently available, is likely the only means of producing a high count rate, high resolution microscope. Nevertheless, this report shows that with existing components, a microscope yielding a count rate of 140 c/s at .4 μ resolution can be constructed.

4. Appendix 1

If the source were a planar emitting surface, each surface point of which emitted isotropically, then from geometrical grounds it is clear that reducing the distance L_{1d} from the condition where $\alpha = \beta$ would have no effect of the atom density at the zone plate, the effect of increased atom flux passing through aperture A_2 being cancelled by the corresponding increase in area over which the atoms were distributed at the zone plate plane. However, given that the emitting surface is neither planar nor the distribution of atom velocities at it's surface isotropic, then a dependence for atom density at the zone plate upon the distance L_{1d} is expected. Unfortunately, in the present example where a high speed ratio source with a small skimmer is used, reducing the distance L_{1d} from 64 cm ($\alpha = \beta$ condition) to 32 cm ($\alpha = 2\beta$) only increases the atom number from 1.10×10^{17} to 1.3×10^{17} m^{-3}. [To calculate the component of the atom number density $n_d{}^*$ at A_2 which delivers atoms onto the zone plate surface for the case when $\alpha = 2\beta$, it must be taken into account that only atoms deriving from the central 50 μ region of the 100 μ skimmer aperture can illuminate the zone plate and hence an effective value of $\xi_{max}{}^* = 1.25 \times 10^{-3}$ rather than $\xi_{max} = 2.5 \times 10^{-3}$ is required in equation (1.6) to obtain the value 1.3×10^{17} m^{-3} presented above. Setting $\alpha > \beta$ also compensates for $\simeq 10\%$ loss in atom density at the zone plate that would occur due to the effects of atom diffraction through aperture A_2, results in a smaller apparatus size and aids in ease of alignment for the zone plate, nozzle and apertures. The price one pays is an increase, by a factor of four, in background pressure in the zone plate chamber.

5. References

[1] Hecht E. and Zajac A., "Optics", Addison-Wesley Publishing Company (1974) 352.

[2] R. B. Doak, "Focussing of an Atomic Beam", submitted for publication (1990).

[3] Knuth, E. L., Notes on Lecture presented at MPI für Strömungsforschung, Göttingen, 30th April 1987 - 21 May 1987.

[4] von Issendorff, B., "Untersuchung und Optimierung von Universal-Ionisationsdetektoren für Molekularstrahlen", Diplomarbeit (1990), pgs. 108-117.

[5] Moore, J. H., Davis, C. D. and Copland, M. A. "Building Scientific Apparatus", Addison-Wesley Publishing Company (1983), pg. 75.